ACADEMIC PRESS

Available online at www.sciencedirect.com
SCIENCE DIRECT®

Journal of Catalysis 213 (2003) 63–72

JOURNAL OF CATALYSIS

www.elsevier.com/locate/jcat

CO vibrational frequencies on methanol synthesis catalysts: a DFT study

J. Greeley,[a] A.A. Gokhale,[a] J. Kreuser,[a] J.A. Dumesic,[a] H. Topsøe,[b] N.-Y. Topsøe,[b] and M. Mavrikakis [a,*]

[a] *Department of Chemical Engineering, University of Wisconsin-Madison, Madison, WI 53706, USA*
[b] *Haldor Topsøe A/S, Nymøllevej 55, DK-2800 Kgs., Lyngby, Denmark*

Received 2 May 2002; revised 3 September 2002; accepted 13 September 2002

Abstract

Periodic, self-consistent density functional theory calculations are used to explain the observed decrease in the vibrational frequency of CO on methanol synthesis catalysts under severe reducing conditions (N.-Y. Topsøe, H. Topsøe, J. Mol. Catal. A Chem. 141 (1999) 95–105). Vibrational frequencies for CO on eight different models of the methanol synthesis catalyst surface have been determined. The calculated vibrational frequency of CO on Cu(111) (1/9 ML CO coverage) with 1/9 ML of Zn adatoms shows a decrease of between 15 and 38 cm^{-1} from the corresponding calculated CO frequency on clean Cu(111) (2073 cm^{-1}). The calculated vibrational frequency of CO on Cu(111) with 1/9 ML of ZnO species shows a decrease of up to 72 cm^{-1} from the CO stretch frequency on clean Cu(111). These calculated CO vibrational frequency decreases agree with the experimentally measured decrease (ca. 50 cm^{-1}), suggesting that Zn and/or ZnO species may be present in the vicinity of active Cu sites of methanol synthesis catalysts under highly reducing conditions. In addition, CO vibrational frequencies on partially oxidized Cu(111) surfaces are shown to increase from the corresponding frequencies on clean Cu(111), in agreement with experimental results.

Keywords: Density functional theory; Catalysis; Methanol; Copper; Zinc; Carbon monoxide

1. Introduction

Copper-based catalysts are used extensively for the synthesis of methanol [1–3]. Typically, copper is dispersed on a support, and the catalyst is promoted with various additives. Accordingly, extensive research has focused on studying the influence that the support and the additives have on the structure of the catalyst and the reaction mechanism [2–10]. It is clear from these studies that the role of the additive depends on the nature of the particular additive, and it is necessary to deal in detail with each specific system. Industrial methanol synthesis catalysts contain ZnO, and special attention has thus been directed toward the understanding of Cu/ZnO-based catalysts [3,5,8,9,11–16].

Over the years there have been conflicting views regarding the structure of Cu/ZnO based catalysts. For example, it has been proposed that copper may be present as copper metal, as Cu^+ species dissolved in ZnO [2,17], as CuZn alloys [18], or as Cu^- at the so-called Schottky junction [8]. Many results, including *in-situ* EXAFS measurements, have indicated that Cu is present as metallic copper [3,12,13,19]. Moreover, it has been shown recently that the Cu/ZnO system may undergo dynamic changes under various reaction conditions. In this respect, it was found that the interaction of metallic Cu particles with ZnO and the resulting Cu particle morphology may depend on the reduction potential of the synthesis gas [13,20]. Such interactions may also give rise to Cu crystals with different amounts of strain [21,22]. Furthermore, the changes in the structure and morphology of the copper particles can result in significant changes in the catalytic activity [20,23].

Previous results [24–26] have suggested that the effects of varying reduction conditions may not be restricted to morphological and structural changes of copper. In fact, recent IR studies [25] have shown large (ca. 50 cm^{-1}) downward CO frequency shifts when CO was adsorbed on Cu/ZnO catalysts reduced under successively more severe conditions. This observation was taken as an indication of the migration of zinc species onto the Cu surfaces under reducing conditions and the formation of possible new surface structures. Low energy scattering (LEIS) experiments [24,27] have also

* Corresponding author.
E-mail address: manos@engr.wisc.edu (M. Mavrikakis).

0021-9517/03/$ – see front matter
PII: S0021-9517(02)00040-4

shown that Zn may segregate toward the surfaces of Cu. Nevertheless, the nature of the Cu–Zn surface structures that may be formed under reducing conditions and whether Zn is present in a metallic or an oxidized state have remainded unclear. For example, such structures may be ascribed to a surface Cu–Zn alloy, as proposed earlier from surface science studies [28]. It is, however, not certain that such structures may be present under actual synthesis conditions. Also, the state of the catalyst appears to be dynamic, and different types of structures may only be dominant features under limited sets of reaction or reduction conditions. There has been a previous attempt to incorporate these features into a dynamic microkinetic description of the methanol synthesis catalysis [23].

Results from recent HRTEM *in-situ* studies [29] provide strong evidence that Cu(111) facets are present in methanol synthesis catalysts. The present study was undertaken to obtain additional insight into the types of clean and modified copper surfaces that may be present under different reaction and reduction conditions. To this end, we have performed DFT calculations for CO adsorbed on various different model surfaces. The CO vibrational frequencies calculated for these cases are compared with those observed experimentally on Cu/ZnO catalysts subjected to different reduction conditions [25]. Based on the results of these comparisons, we suggest that under mildly reducing conditions Cu(111) surfaces may dominate, whereas under more severe reduction conditions the surfaces may contain zinc adspecies (as Zn or ZnO moieties). These structures are different from those in bulk and surface alloys. Strain effects, which may also be present, do not appear to be the origin of the observed IR frequency shifts. Finally, partial oxidation of the Cu(111) surfaces leads to an increase in the CO vibrational frequency, in agreement with experimental results.

2. Methods

Self-consistent periodic slab calculations [30] based on gradient-corrected density functional theory (DFT) were carried out using DACAPO, the total energy calculation code [31]. A three-layer slab of Cu is used, periodically repeated in a supercell geometry with five equivalent layers of vacuum between any two successive metal slabs. Calculations are performed on 2×2 (surface coverage of $1/4$ ML) and 3×3 (surface coverage of $1/9$ ML) unit cells with the top metal layer relaxed in each case. Adsorption is allowed on only one of the two surfaces exposed, and the electrostatic potential is adjusted accordingly [32]. Ionic cores are described by ultrasoft pseudopotentials [33], and the Kohn–Sham one-electron valence states are expanded in a basis of plane waves with kinetic energy below 25 Ry. The surface Brillouin zone is sampled at 18 special **k** points. In all cases, convergence of the total energy with respect to the **k**-point set, energy cutoff, and the number of metal layers included is confirmed. The exchange–correlation energy and potential are described by the generalized gradient approximation (GGA-PW91) [34,35]. The self-consistent PW91 density is determined by iterative diagonalization of the Kohn–Sham Hamiltonian, Fermi population of the Kohn–Sham states ($k_BT = 0.1$ eV), and Pulay mixing of the resulting electronic density [36]. All total energies have been extrapolated to $k_BT = 0$ eV. The calculated heat released upon adsorption of CO on the surfaces examined is termed the CO binding energy (BE) in the remainder of this paper.

The calculated gas-phase bond energy for CO(g) is 10.96 eV, in agreement with the experimental value of 11.16 eV at 298 K [37]. The lattice constant for bulk Cu is found to be 3.66 Å, in agreement with the experimental value of 3.615 Å [37]. Similarly, the lattice constant for bulk Cu_3Zn is calculated to be 3.47 Å, in agreement with the experimental value of 3.66 Å [38]. Vibrational frequencies for the adsorbed CO states are estimated by fixing the C–O geometric center and displacing the C and O atoms along the C–O bond axis. A harmonic potential energy surface is fit to the resulting total energy values. In the calculations for stretched surfaces, the lattice is stretched in both directions of the surface plane, but the direction perpendicular to the surface plane is kept at its bulk, equilibrium separation. This approach has been shown to give a good estimate for the effect of strain on the thermochemistry and kinetics of surface reactions on transition metal surfaces [22,39].

Current DFT methods find fcc as the best site for CO adsorption on many transition metals, whereas experiments suggest the top site to be the preferred site [40–42]. For this reason, and for the purposes of this study, we have focused our attention on top sites only.

3. Results

Results are reported in Table 1 for the binding energy and vibrational stretching frequency of CO adsorbed on various model catalyst surfaces based on Cu(111). A description of the results of these calculations is presented below for different scenarios representing the adsorption sites for catalysts involving copper supported on zinc oxide.

3.1. CO on Cu(111)

The binding energy for CO on a top site on this surface is calculated to be -0.70 eV at $\theta = 1/4$ ML, and the vibrational frequency is 2093 cm^{-1}. At $\theta = 1/9$ ML, the BE is -0.69 eV, and the vibrational frequency is 2073 cm^{-1}. We note that the calculated binding energies and vibrational frequencies for CO adsorbed on Cu(111) serve as reference points for the comparison in Table 1 with results calculated for CO adsorbed on surfaces that have been altered from Cu(111).

Table 1
Summary of calculated binding energies (BE) and vibrational frequencies for CO on different model methanol synthesis catalysts

Model	Description	θ (ML)	BE	Vibrational frequencies	Shift in vibrational frequency w.r.t. reference state
	Reference State Cu(111) unstrained	**1/4**	**−0.70 eV**	**2093 cm^{-1}**	–
		1/9	**−0.69 eV**	**2073 cm^{-1}**	–
1	O adatom on Cu(111)	1/4	−0.84 eV	2158 cm^{-1}	65 cm^{-1}
2	Subsurface oxygen	1/4	−1.13 eV	2127 cm^{-1}	34 cm^{-1}
3	Cu(111) under strain	1/4	−0.66 to −0.85 eV	2070 to 2128 cm^{-1}	−23 to 35 cm^{-1}
4a	Cu adatoms on Cu(111) (hcp)	1/4	−1.16 eV	2132 cm^{-1}	39 cm^{-1}
4b	Cu adatoms on Cu(111) (fcc)	1/4	−1.16 eV	2128 cm^{-1}	35 cm^{-1}
5	Cu_3Zn(111) bulk alloy	1/4	−0.39 eV	2101 cm^{-1}	8 cm^{-1}
6	Cu_3Zn surface alloy on top of Cu(111)	1/4	−0.62 eV	2089 cm^{-1}	−4 cm^{-1}
7a	Zn adatoms on Cu(111) (hcp)	1/4	−0.34 eV	1924 cm^{-1}	−169 cm^{-1}
		1/9	−0.64 eV	2035 cm^{-1}	−38 cm^{-1}
7b	Zn adatoms on Cu(111) (fcc)	1/4	−0.40 eV	1952 cm^{-1}	−141 cm^{-1}
		1/9	−0.64 eV	2058 cm^{-1}	−15 cm^{-1}
8	ZnO/Cu(111)	1/4	−0.35 eV	1470 cm^{-1}	−623 cm^{-1}
		1/9	−0.63 to −0.66 eV	2001 to 2083 cm^{-1}	−72 to 10 cm^{-1}

Reference states are bold-faced. For comparison, experimental results [25] suggest a decrease of CO vibrational frequency by ~ 50 cm^{-1} under various catalyst reducing conditions.

3.2. CO on Cu(111) with O adatoms

In an effort to study the effect of surface oxygen on the vibrational frequency of CO on Cu(111), 1/4 ML of carbon monoxide was adsorbed onto a surface consisting of 1/4 ML of surface oxygen on Cu(111). This configuration could serve as an approximate model of partially oxidized copper sites on methanol synthesis catalysts. CO adsorbed at the top site with the O adatom at the farthest fcc site (Fig. 1) was found to be the most stable configuration, with a CO binding energy of −0.84 eV. The CO vibrational frequency in this case was found to be 2158 cm^{-1}.

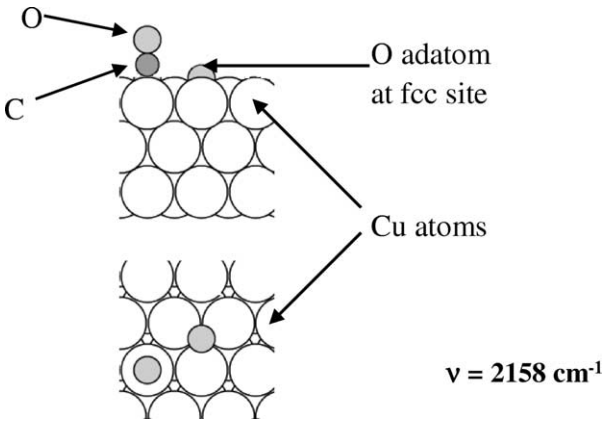

Fig. 1. CO adsorbed onto Cu(111) ($\theta_{CO} = 1/4$ ML) with oxygen adatoms at fcc sites ($\theta_O = 1/4$ ML). Top and bottom panels provide a cross-section and a on-top view, respectively. The CO molecule is perpendicular to the surface plane.

3.3. CO on Cu(111) containing subsurface oxygen

A modified surface for CO adsorption was formed by placing 1/4 ML of subsurface oxygen between the first and second copper layers of a Cu(111) surface and allowing the surface to relax, thus capturing a limited set of local surface reconstruction effects. The most favorable CO adsorption configuration in this situation is on top of a Cu atom adjacent to the subsurface oxygen (Fig. 2). In this situation, the surface Cu atom bonded to CO is pulled out of the surface

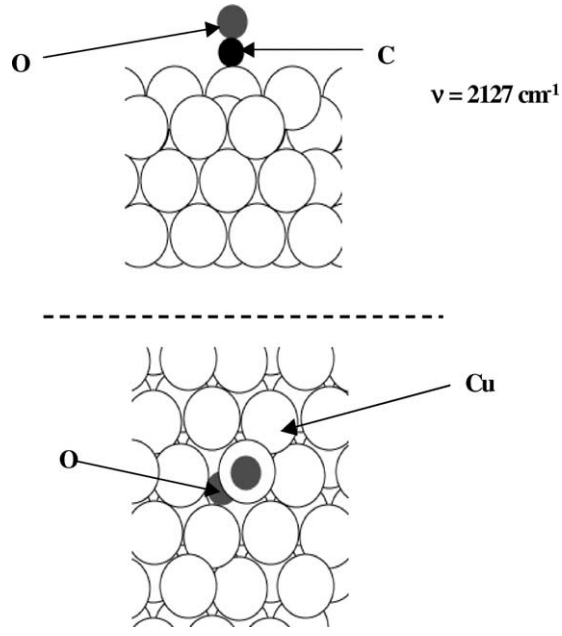

Fig. 2. CO adsorbed onto Cu(111) with 1/4 ML subsurface oxygen. A cross-section and an on-top view are provided. The CO molecule is perpendicular to the surface plane.

by 0.68 Å by the adsorbed CO. The binding energy of CO is −1.13 eV, and the associated vibrational frequency is 2127 cm^{-1}. The binding energy decreases to −1.01 eV when all Cu atoms are frozen in their relaxed positions and the subsurface oxygen is removed, and the vibrational frequency remains constant.

3.4. CO on strained Cu(111)

A variety of effects could lead to strains fields in supported copper particles. Accordingly, lateral strains of between −7.5 and +9.0% were introduced into the Cu(111) slabs by increasing the lattice parameter with a 2×2 unit cell (and allowing the surfaces to relax). These strain values are physically reasonable, since they are comparable to the strains induced in Cu layers by 1/4 ML of subsurface oxygen (see above). The binding energies for CO on top sites and the associated vibrational frequencies were calculated for five different strain values (including the equilibrium, unstrained surface) between these two limits. For extreme compression (−7.5%), adsorbed CO pulls a copper atom up from the Cu(111) plane by 0.67 Å, and the binding energy is −0.75 eV. The magnitude of the binding energy decreases at lower compression and the Cu atom bonded to CO is pulled to a lesser extent from the surface. As the surface then becomes stretched, the magnitude of the binding energy increases (Fig. 3). The vibrational frequency on the highly compressed surface is 2128 cm^{-1}. The frequency remains nearly constant between 2085 and 2095 cm^{-1} as the surface is stretched and Cu is no longer pulled from the surface to a significant extent by adsorbed CO (Fig. 3).

3.5. CO on Cu(111) with Cu adatoms

Carbon monoxide was adsorbed onto a surface consisting of 1/4 ML of Cu-adatoms placed on a Cu(111) surface. The most favorable positions for depositing the Cu adatoms are the fcc and hcp sites. Carbon monoxide prefers to adsorb on top of the adatoms, with a BE of −1.16 eV. The calculated vibrational frequency for these adsorbed CO states is ca. 2130 cm^{-1}.

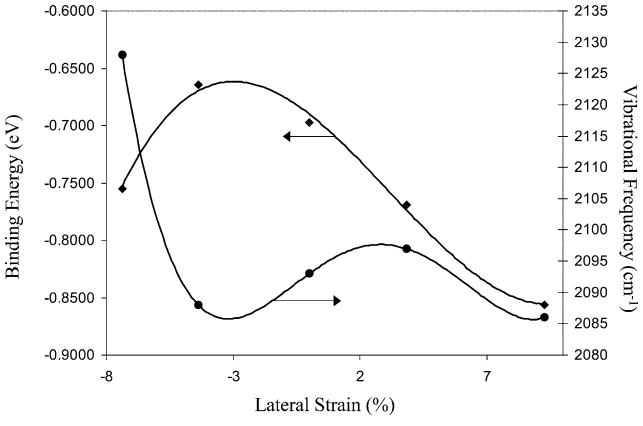

Fig. 3. Binding energy and vibrational frequency of CO ($\theta = 1/4$ ML) as a function of the percent lateral strain of Cu(111). Surface relaxation was allowed only in the direction perpendicular to the surface plane. More negative binding energies mean stronger binding.

3.6. CO on Cu_3Zn(111) and on a Cu_3Zn(111) overlayer over Cu(111)

The low symmetry of Cu_3Zn(111) leads to a higher number of possible adsorption sites. Calculations were performed on the 13 sites shown in Fig. 4. No stable adsorbed CO was found on top on Zn atoms. Adsorption of CO on top of copper atoms of the Cu_3Zn(111) alloy surface is exothermic, with a binding energy of −0.39 eV. The vibrational frequency of CO adsorbed on top of Cu sites is 2101 cm^{-1}.

Zinc atoms were placed substitutionally at 1/4 ML in the surface layer of a Cu(111) slab, since results from DFT calculations indicate that Zn is more stable in the surface layer than in the subsurface layer by about 0.3 eV/Zn atom. The adsorption of CO on this Cu_3Zn surface deposited on Cu(111) shows a strong preference for binding to Cu atoms, with a binding energy of −0.62 eV. The vibrational frequency of CO in this configuration is 2089 cm^{-1} (Fig. 5).

3.7. CO on Cu(111) with Zn adatoms

Carbon monoxide was adsorbed onto surfaces consisting of 1/4 ML and 1/9 ML of Zn-adatoms placed on a Cu(111) surface at fcc and hcp sites. Adsorption of CO on top of Zn adatoms is energetically unfavorable, whereas adsorption of CO on top of Cu atoms β to Zn (Fig. 6) is exothermic. At 1/4 ML coverage, the binding energies for CO adsorption are −0.34 and −0.40 eV for Zn adatoms located at hcp and fcc sites, respectively. The CO vibrational frequencies in these cases are 1924 and 1952 cm^{-1}. At 1/9 ML coverage, the binding energy for CO adsorption is −0.64 eV for Zn adatoms located at either fcc or hcp sites. The calculated vibrational frequencies are 2058 and 2035 cm^{-1} for the cases where Zn adatoms are located at fcc and hcp sites, respectively.

3.8. CO on Cu(111) with ZnO adspecies

Carbon monoxide was adsorbed on surfaces consisting of 1/4 and 1/9 ML of ZnO adspecies placed on a Cu(111) surface. The ZnO has several stable configurations on this surface (Fig. 7). Calculations were performed for the most stable configuration of ZnO on Cu(111), corresponding to the situation where Zn adatoms are located at hcp sites and oxygen adatoms are located at fcc sites—ZnhcpOfcc (see Fig. 7). While two stable sites for CO adsorption were found for this case, corresponding to hcp and top sites of Cu, we have focused attention on the top adsorbed configuration. The interaction of CO with Cu atoms located near the ZnO adspecies gives rise to an adsorbed CO molecule that is tilted by 51° with respect to the surface normal. The

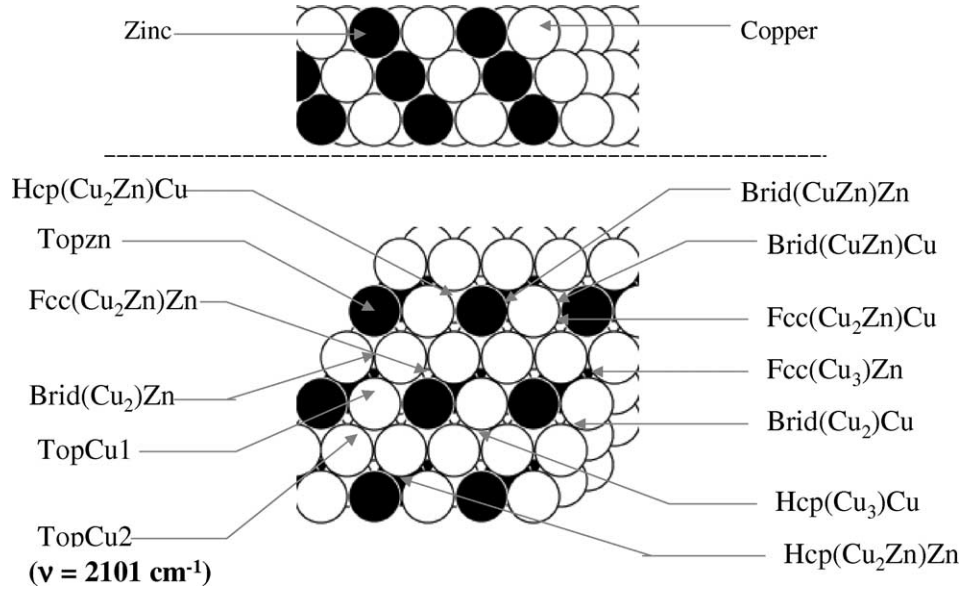

Fig. 4. The distinct sites on the surface of a $Cu_3Zn(111)$ bulk alloy studied for CO adsorption. A cross-section and an on-top view are provided. The symbols in parenthesis indicate the atomic composition of the surface site and the symbols following the parentheses indicate the nature of the atom below the site in the second or the third layer, as appropriate. CO adsorbed at the TopCu1 and TopCu2 sites is perpendicular to the surface plane.

binding energy and vibrational frequency are −0.35 eV and 1470 cm^{-1}, respectively, at a coverage of 1/4 ML. When the coverage decreases to 1/9 ML, the most favorable top configurations for adsorbed CO have stronger binding energies of −0.63, −0.65, and −0.66 eV (Fig. 8). The adsorbed CO species are tilted with respect to the normal in the case of the first two sites by 14° and 6°, respectively, while for the third case CO is perpendicular to the surface. The corresponding vibrational frequencies are 2053, 2001, and 2083 cm^{-1}, respectively.

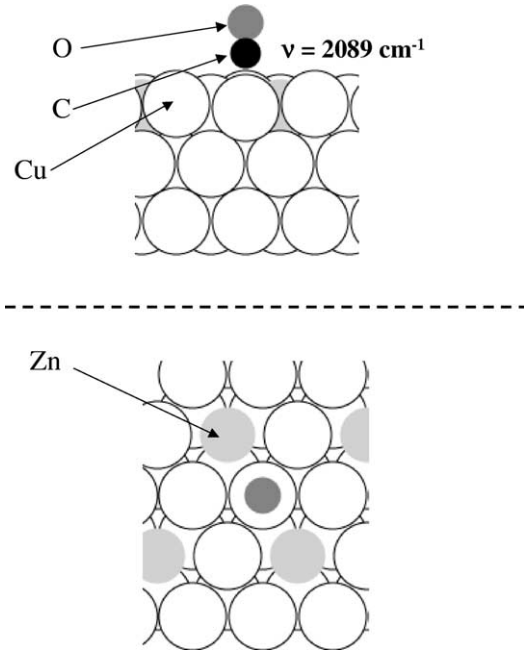

Fig. 5. CO adsorption on a Cu_3Zn monolayer on top of a Cu(111) surface. A cross-section and an on-top view are provided. The CO molecule is perpendicular to the surface plane.

4. Discussion

Results from TPD studies [43–46] have generally found CO desorption peaks at 160–170 K on Cu(111), corresponding to CO desorption energies from about 0.44 to 0.52 eV (using a standard Redhead analysis). Vibrational studies of CO on Cu(111) [43,47–49] give C–O stretching frequencies in the range of 2070–2078 cm^{-1}, and these results are taken to indicate that top site adsorption is the dominant adsorption mode for CO on Cu(111). Additionally, vibrational frequencies of 2085 and 2096 cm^{-1} have been measured for CO adsorbed onto Cu/ZnO samples reduced at the relatively low temperature of 490 K [25]. Our calculated BE at $\theta = 1/9$ ML (−0.69 eV) is about 0.2 eV higher than the reported experimental estimates (it is, however, in reasonable agreement with a BE of −0.79 eV found for CO at an fcc site using periodic DFT calculations [41]—top site adsorption was not considered in that study). This difference between the calculated and the experimentally determined CO BE is reasonable, since the PW91 functional may overpredict binding energies [30,31]. Importantly, the calculated vibrational frequency from our study (2073 cm^{-1}) is in good agreement with the experimental values, indicating that the vibrational results from DFT calculations are of sufficient accuracy to make meaningful comparisons between

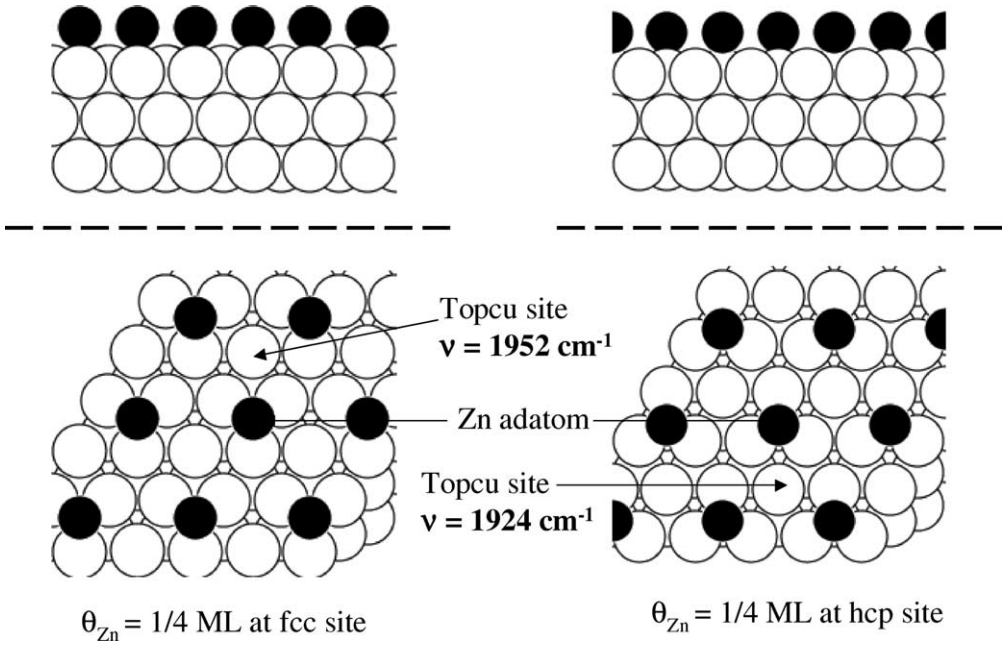

Fig. 6. Adsorption sites of CO for $\theta_{CO} = 1/4$ ML on a Cu(111) slab with $\theta_{Zn} = 1/4$ ML with Zn adatoms at fcc and hcp positions. A cross-section and an on-top view are provided. CO adsorbed at the Topcu sites is perpendicular to the surface plane.

different model surfaces. We note that previous authors have found no correlation between binding energy and CO stretch frequency on the (111) surfaces of platinum and platinum–ruthenium alloys [50,51]. These studies, in agreement with the results presented above, demonstrate that frequency and binding energy results are essentially independent of one another and that good vibrational frequency results can be found even when binding energy estimates contain modest errors.

4.1. CO on Cu(111) with O adatoms

The calculated binding energy and frequency for CO in this model are −0.84 eV and 2158 cm^{-1}. This frequency exactly matches the weak and reversible spectra detected by Scarano et al. [52]. Topsøe and Topsøe [25] have also found frequencies of 2155 and 2139 cm^{-1}, which they attribute to CO adsorbed on Cu^{2+} (Cu/SiO_2) and Cu^+ (Cu/Al_2O_3). Our data agree well with these experimental

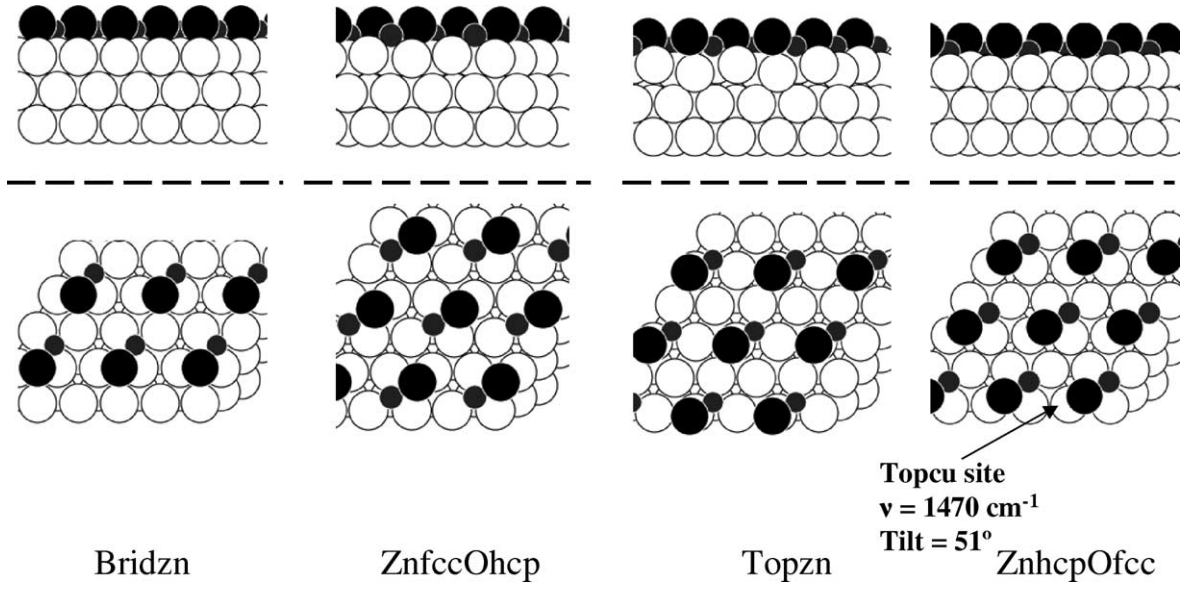

Fig. 7. The different stable configurations for $\theta_{ZnO} = 1/4$ ML adsorption on Cu(111). Configuration ZnhcpOfcc is the most stable. Cross-section and on-top views are provided. The tilt of CO with respect to the surface normal is given in (°). 0° corresponds to a CO molecule perpendicular to the surface.

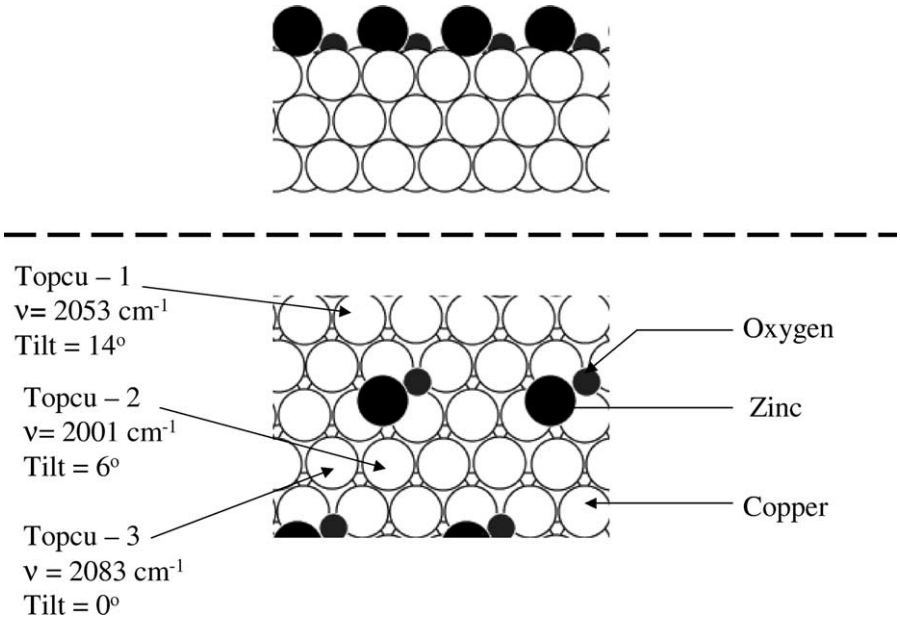

Fig. 8. Stable top sites for CO adsorption on ZnO/Cu(111) ($\theta_{CO} = 1/9$ ML and $\theta_{ZnO} = 1/9$ ML). The Topcu2 site gives the most pronounced downward shift, 72 cm^{-1}, with respect to the reference state frequency of 2073 cm^{-1}. The Topcu1 site gives a downward shift of 20 cm^{-1}. The tilt of CO with respect to the surface normal is given in (°). 0° corresponds to a CO perpendicular to the surface. A cross-section and an on-top view are provided.

values, supporting the idea that CO vibrational frequencies increase on oxidized copper surfaces. The calculated values of the binding energy and the CO stretching frequency are higher than those determined on Cu(111) with an equivalent coverage of CO (−0.70 eV and 2093 cm^{-1}). The increased CO BE points to an additional stabilization of CO due to the presence of coadsorbed surface oxygen.

4.2. CO on Cu(111) containing subsurface oxygen

The calculated binding energy and frequency for CO in this model are −1.13 eV and 2127 cm^{-1}. The frequency agrees well with a frequency of 2127 cm^{-1} measured on Cu_2O(111) [52] and with the results of Topsøe and Topsøe [25] (2132 cm^{-1}, tentatively assigned to Cu^+ on Cu/SiO_2). As in the previous case, the calculated values of the binding energy and the CO stretching frequency are higher than the values of these quantities on Cu(111) (−0.70 eV and 2093 cm^{-1}). The increase in CO stretching frequency caused by subsurface oxygen species suggests that these species are not responsible for the shift to lower frequencies seen by Topsøe and Topsøe [25] under severe reducing conditions.

Adsorption of CO on Cu(111) with 1/4 ML subsurface oxygen lifts the Cu atom substantially above the surface (by 0.67 Å), reminiscent of the effect observed in the case of H on Pt [53]. It is interesting to note that the CO stretching frequency calculated in the presence of subsurface oxygen is the same as the frequency calculated with the subsurface oxygen removed and the surface frozen in its respective corrugated position; the binding energy shows a modest change (from −1.13 to −1.01 eV) between these two situations. This suggests that subsurface oxygen is, to a large extent, electrostatically screened by the deformed Cu(111) layer above it, leaving primarily the strain in the deformed Cu(111) layer to influence the CO binding properties. Thus, the change in CO frequency induced by subsurface oxygen appears to be largely a geometric, rather than an electronic, effect.

4.3. CO on strained Cu(111)

Giorgio et al. found a maximum strain of ∼ 12% in the case of Au particles on anatase (TiO_2) [54]. Therefore, we have chosen to investigate Cu(111) surfaces with lateral strains between −7.5% (compression) and +9.0% (stretching), well within this experimentally reported value. Figure 3 shows that strain has a considerable, yet nonmonotonic, effect on the CO binding energy. The increase in the CO binding energy magnitude with positive strain is analogous to the increase observed in the presence of subsurface oxygen, suggesting that strain effects are important in the modification of Cu(111) surfaces by subsurface oxygen. Also, increases in binding energy for highly stretched surfaces have been calculated previously for CO and NO on Ru(0001) [39,55] and for O on Cu(111) [22], providing indirect support for our conclusion that the binding energy increases with high strain levels on Cu(111). At the highest compressions examined, the Cu atom beneath CO is lifted out of the surface, resulting in a quasi-adatom configuration which is responsible for an increase in the CO BE calculated for that range of compression.

Figure 3 also shows the variation of the CO vibrational frequency with strain. At the highest compression value, a large increase in frequency, likely resulting from the quasi-adatom effect mentioned above, is observed. Excluding this

value from the analysis, the data in Fig. 3 might indicate, within a certain range of strain values, a modest increase in frequency with strain, consistent with the results of Kampshoff et al. [56]. In any case, it appears that strain effects are an unlikely explanation for the experimentally observed IR frequency decrease [25].

4.4. CO on Cu(111) with Cu adatoms

The stretching frequency calculated for CO adsorbed on Cu adatoms located on Cu(111) is about 40 cm^{-1} higher than that for CO on Cu(111). Therefore, it is unlikely that Cu adatoms are responsible for the experimentally observed frequency decrease. The binding energy of CO is -1.16 eV, which is considerably higher than that for Cu(111). Interestingly, the frequency and binding energy for CO adsorbed on Cu adatoms are nearly identical to the corresponding values for the Cu(111) surface with subsurface oxygen. The values are also similar to those on the highly compressed Cu(111) surface. The agreement between the results for CO adsorption on Cu adatoms, CO adsorption on compressed Cu(111) surfaces, and CO adsorption on surfaces containing subsurface oxygen can be explained by the observation that CO pulls a copper atom up from the surface in these latter two cases. Thus, all three cases correspond to the situation where CO is adsorbed on a copper atom that is above the surface.

4.5. CO on $Cu_3Zn(111)$ and on a $Cu_3Zn(111)$ overlayer on Cu(111)

The binding energy of CO on top of Cu atoms adjacent to Zn on the (111) surface of a Cu_3Zn bulk alloy is -0.39 eV, and the calculated vibrational frequency is 2101 cm^{-1}. This frequency is slightly higher than the corresponding frequency for CO on Cu(111), indicating that this model is an unlikely explanation for the experimental frequency decrease at high reduction temperatures.

The most favorable top site for CO adsorption on a $Cu_3Zn(111)$ overlayer on Cu(111) is on copper atoms. The binding energy for CO adsorption and the CO stretching frequency for this case are similar to the values for CO on Cu(111). Therefore, it is unlikely that the formation of a Zn/Cu surface alloy can explain a significant decrease in the CO vibrational frequency.

4.6. CO on Cu(111) with Zn adatoms

Adsorption of CO at positions β to Zn adatoms on fcc sites of a Cu(111) surface for a coverage of 1/4 ML is exothermic by 0.4 eV, and adsorption at positions γ to Zn on Cu(111) for a coverage of 1/9 ML is exothermic by 0.64 eV (Fig. 6). These values agree with binding energies of CO estimated by Giamello et al. [57] with microcalorimetry on reduced Cu/ZnO. These authors estimated a binding energy of between -0.43 and -0.52 eV at high coverages and between -0.65 and -0.78 eV at low coverages. Importantly, we find in the present study that the CO stretching frequency shifts to lower values, compared to Cu(111), by between -140 cm^{-1} and -169 cm^{-1} at a coverage of 1/4 ML and by between -15 cm^{-1} and -38 cm^{-1} at a coverage of 1/9 ML. These frequency shifts indicate that Zn adatoms may, indeed, be present on the surface of methanol synthesis catalysts under highly reducing conditions, as probed by Topsøe and Topsøe in their experiments [25].

4.7. CO on Cu(111) with ZnO adspecies

Adsorption of CO on top of Cu atoms adjacent to ZnO adspecies at a coverage of 1/4 ML shows a significant tilt (51°) of the CO axis with respect to the surface normal accompanied by a large downward frequency shift (~ 600 cm^{-1}) compared to CO on Cu(111). At a lower coverage of 1/9 ML, the stretching frequencies for CO adsorbed on three atop Cu sites (Fig. 8) are equal to 2001, 2053, and 2083 cm^{-1}. The lowest of these frequencies involves a CO molecule tilted slightly away from the surface normal (6°), and it corresponds to a downward shift of 72 cm^{-1} compared to CO adsorbed on Cu(111). These results suggest that ZnO may also be present on methanol synthesis catalyst surfaces under severely reducing conditions. Similar sites could be envisioned at the interface of copper particles with ZnO supports.

4.8. Relevance of models to methanol synthesis catalysts

Of the various models considered in this study, the results for Zn and ZnO adspecies on Cu(111) most clearly reproduce the experimentally observed decrease in CO vibrational frequency with increasing reduction temperature [25]. Hence, our results suggest that Zn and/or ZnO species may be present on copper particles in Cu/ZnO methanol synthesis catalysts under highly reducing conditions. This conclusion is supported by recent LEIS studies of Viitanen et al. [27] where it was found that Zn enrichment in the surface region of $Cu/ZnO/SiO_2$ catalysts was more pronounced at high reducing temperatures. Indirect support for the conclusion comes from several studies that have shown a link between Zn or ZnO species on copper surfaces and methanol synthesis activity. The activity measurements in these studies were performed under reducing conditions (hydrogen-rich atmospheres at 220–300 °C, very similar to the highly reducing conditions employed by Topsøe and Topsøe [25]), and the Zn or ZnO species were likely present on the catalyst surfaces under such conditions. For example, Curry-Hyde et al. [15] found a correlation between methanol synthesis activity and the loading of ZnO on the surface of leached catalyst pellets. Fujitani et al. have shown that Zn deposited on Cu(111) leads to dramatic increases in methanol synthesis rates [28,58]. Fujitani et al. also determined, using XPS, that formate species (thought to be involved in methanol synthesis) are stabilized by surface Zn and hence may be more

likely to react to methanol in the presence of Zn species. Morikawa et al. [59] concluded from periodic DFT calculations that formate is likely to lift Zn atoms out of the Cu(111) surface layer into an adatom-type situation.

Various researchers have suggested that CuZn alloys or surface alloys may be formed on methanol synthesis catalysts under highly reducing conditions. Grunwaldt et al. [20] observed CuZn alloys with EXAFS under severely reducing conditions. Fujitani and Nakamura [9] found evidence for CuZn alloy formation with XRD. Morikawa et al. [59] calculated that CuZn surface alloys are more stable than Zn adatoms on Cu(111). While CuZn alloy or surface alloys may exist, the results from our DFT calculations suggest that these structures do not lead to significant downward shifts in CO vibrational frequencies. Thus, it appears that the downward shifts observed experimentally are most likely caused by the presence of Zn and/or ZnO adspecies on the surface of copper (and perhaps CuZn alloy) particles, or at Cu sites close to the metal–support interface.

Finally, it is encouraging to notice the generally good agreement of experimental and theoretical CO stretch frequencies on both clean and partially oxidized copper surfaces. This agreement legitimizes the use of theory for screening potential configurations of the active sites of methanol synthesis catalysts.

5. Conclusions

Generally good agreement of experimental and theoretical CO stretch frequencies on both clean and partially oxidized copper surfaces has been found in the present study. This agreement justifies the use of theory for screening potential configurations of the active sites of methanol synthesis catalysts under experimental conditions. It has been found experimentally that the CO vibrational frequency on Cu/ZnO methanol synthesis catalysts shifts downward by about 50 cm^{-1} as the reducing temperature of the catalyst is increased. In an attempt to explain this observation, the CO binding energies and vibrational frequencies have been calculated using periodic DFT methods for CO adsorbed on various models for surface structures on Cu/ZnO catalysts. A vibrational downshift of up to 72 cm^{-1} has been calculated for CO adsorbed adjacent to ZnO adspecies ($\theta_{ZnO} = \theta_{CO} = 1/9$ ML) on Cu(111), and downshifts between 15 and 38 cm^{-1} have been found for CO adsorbed near Zn adatoms ($\theta_{Zn} = \theta_{CO} = 1/9$ ML). In contrast, significant downward shifts in the vibrational frequency are not found for stretched/compressed Cu(111) surfaces, for Cu-adatoms on Cu(111), for Cu_3Zn(111) alloy surfaces, for Cu_3Zn(111) overlayers on Cu(111), and for Cu(111) containing surface or subsurface oxygen. Accordingly, the downward shifts of the CO vibrational frequency observed experimentally are most likely caused by the presence of Zn and/or ZnO adspecies on the surface of copper (and perhaps CuZn alloy) particles or at sites close to the metal–support interface under highly reducing conditions.

Acknowledgments

J.G. acknowledges partial financial support from a National Science Foundation predoctoral fellowship. M.M. acknowledges partial financial support from an NSF-CAREER award (CTS-0134561) and a Shell Oil Company Foundation Faculty Career Initiation Award. J.G., A.G., and M.M. acknowledge partial support from the National Energy Research Scientific Computing Center (NERSC) through the DOE-BES office. Additional computational resources were provided by the National Partnership for Advanced Computational Infrastructure (NPACI) under NSF cooperative agreement ACI-9619020. BP Amoco is thanked for an equipment grant.

References

[1] J.B. Hansen, Handbook of Heterogeneous Catalysis, Vol. 4, Wiley–VCH, New York, 1997.
[2] K. Klier, Adv. Catal. 31 (1982) 243.
[3] K.C. Waugh, Catal. Today 15 (1992) 51.
[4] R. Burch, S.E. Golunski, M.S. Spencer, Catal. Lett. 5 (1990) 55.
[5] M.S. Spencer, Catal. Lett. 50 (1998) 37.
[6] B.S. Clausen, J. Schiotz, L. Grabek, C.V. Ovesen, K.W. Jacobsen, J.K. Nørskov, H. Topsøe, Top. Catal. 1 (1994) 367.
[7] A. Gotti, R. Prins, J. Catal. 178 (1998) 511.
[8] J.C. Frost, Nature 334 (1988) 577.
[9] T. Fujitani, J. Nakamura, Catal. Lett. 56 (1998) 119.
[10] J. Nerlov, I. Chorkendorff, J. Catal. 181 (1999) 271.
[11] G.C. Chichen, K.C. Waugh, D.A. Whan, Appl. Catal. 25 (1986) 101.
[12] J. Yoshihara, C.T. Campbell, J. Catal. 161 (1996) 776.
[13] B.S. Clausen, B. Lengeler, B.S. Rasmussen, W. Niemann, H. Topsøe, J. Phys. Colloq. C 8 (1) (1986) 237.
[14] K.D. Jung, O.S. Joo, S.H. Han, Catal. Lett. 68 (2000) 49.
[15] H.E. Curry-Hyde, M.S. Wainwright, D.J. Young, Applied Catalysis 77 (1991) 75.
[16] H.E. Curry-Hyde, M.S. Wainwright, D.J. Young, Applied Catalysis 77 (1991) 89.
[17] V. Ponec, Surf. Sci. 272 (1992) 111.
[18] I. Nakamura, H. Nakano, T. Fujitani, T. Uchijima, J. Nakamura, Surf. Sci. 402–404 (1998) 92.
[19] T.H. Fleisch, R.L. Mieville, J. Catal. 90 (1984) 165.
[20] J.D. Grunwaldt, A.M. Molenbroek, N.-Y. Topsøe, H. Topsøe, B.S. Clausen, J. Catal. 194 (2000) 452.
[21] M.M. Günter, T. Ressler, B. Bems, C. Büscher, T. Genger, O. Hinrichsen, M. Muhler, R. Schlögl, Catal. Lett. 71 (2001) 37.
[22] Y. Xu, M. Mavrikakis, Surface Science 494 (2001) 131.
[23] C.V. Ovesen, B.S. Clausen, J. Schiotz, P. Stolze, H. Topsøe, J.K. Nørskov, J. Catal. 168 (1997) 133.
[24] D.S. Brands, E.K. Poels, T.A. Krieger, O.V. Makarova, C. Weber, S. Veer, A. Bliek, Catal. Lett. 36 (1996) 175.
[25] N.-Y. Topsøe, H. Topsøe, J. Mol. Catal. A Chem. 141 (1999) 95.
[26] Y.B. Kagan, L.G. Liberov, E.V. Slivinskii, S.M. Loktev, G.I. Lin, A.Y. Rozovskii, A.N. Bashkirov, Dokl. Akad. Nauk SSSR 221 (1975) 1093.
[27] M.M. Viitanen, W.P.A. Jansen, R.G. van Welzenis, H.H. Brongersma, D.S. Brands, E.K. Poels, A. Bliek, J. Phys. Chem. B 103 (1999) 6025.
[28] I. Nakamura, T. Fujitani, T. Uchijima, J. Nakamura, J. Vac. Sci. Technol. A 14 (1996) 1464.
[29] P.L. Hansen, J.B. Wagner, S. Helveg, J.R. Rostrup-Nielsen, B.S. Clausen, H. Topsøe, Science 295 (2002) 2053.
[30] J. Greeley, J.K. Nørskov, M. Mavrikakis, Ann. Rev. Phys. Chem. 53 (2002) 319.

[31] B. Hammer, L.B. Hansen, J.K. Nørskov, Phys. Rev. B 59 (1999) 7413.
[32] J. Neugebauer, M. Scheffler, Phys. Rev. B 46 (1992) 16067.
[33] D. Vanderbilt, Phys. Rev. B 41 (1990) 7892.
[34] J.P. Perdew, J.A. Chevary, S.H. Vosko, K.A. Jackson, M.R. Pederson, D.J. Singh, C. Fiolhais, Phys. Rev. B 46 (1992) 6671.
[35] J.A. White, D.M. Bird, Phys. Rev. B 50 (1994) 4954.
[36] G. Kresse, J. Furthmuller, Comput. Mater. Sci. 6 (1996) 15.
[37] CRC Handbook of Chemistry and Physics, 76th ed., CRC Press, New York, 1996.
[38] P. Villers, L.D. Calvert, Pearson's Handbook of Crystallographic Data for Intermetallic Phases, 2nd ed., ASTM International, Newbury, OH, 1991.
[39] M. Mavrikakis, B. Hammer, J.K. Nørskov, Phys. Rev. Lett. 81 (1998) 2819.
[40] P. Feibelman, B. Hammer, J. Nørskov, F. Wagner, M. Scheffler, R. Stumpf, R. Watwe, J. Dumesic, J. Phys. Chem. B 105 (2001) 4018.
[41] J. Greeley, M. Mavrikakis, J. Catal. 208 (2002) 291.
[42] J. Greeley, M. Mavrikakis, J. Am. Chem. Soc. 124 (2002) 7193.
[43] P. Hollins, J. Pritchard, Surf. Sci. 89 (1979) 486.
[44] W. Kirstein, B. Krüger, F. Thieme, Surf. Sci. 176 (1986) 505.
[45] I. Bönicke, W. Kirstein, S. Spinzig, F. Thieme, Surf. Sci. 313 (1994) 231.
[46] S. Kneitz, J. Gemeinhardt, H.P. Steinrück, Surf. Sci. 440 (1999) 307.
[47] B.E. Hayden, K. Kretzchmar, A.M. Bradshaw, Surf. Sci. 155 (1985) 553.
[48] R. Raval, S.F. Parker, M.E. Pemble, P. Hollins, J. Pritchard, M.A. Chesters, Surf. Sci. 203 (1988) 353.
[49] J.K. Eve, E.M. McCash, Chem. Phys. Lett. 313 (1999) 575.
[50] M.T.M. Koper, T.E. Shubina, R.A. van Santen, J. Phys. Chem. B 106 (2002) 686.
[51] S.A. Wasileski, M.J. Weaver, M.T.M. Koper, J. Electroanal. Chem. 500 (2000) 344.
[52] D. Scarano, S. Bordiga, C. Lamberti, G. Spoto, G. Ricchiardi, A. Zecchina, C.O. Areán, Surf. Sci. 411 (1998) 272.
[53] S. Horch, H.T. Lorensen, S. Helveg, E. Laegsgaard, I. Stensgaard, K.W. Jacobsen, J.K. Nørskov, F. Besenbacher, Nature 398 (1999) 134.
[54] S. Giorgio, C.R. Henry, B. Pauwels, G. van Tendeloo, Mat. Sci. Eng. A 297 (2001) 197.
[55] J. Wintterlin, T. Zambelli, J. Trost, M. Mavrikakis, J. Greeley, submitted.
[56] E. Kampshoff, E. Hahn, K. Kern, Phys. Rev. Lett. 73 (1994) 704.
[57] E. Giamello, B. Fubini, P. Lauro, Appl. Catal. 21 (1986) 133.
[58] T. Fujitani, I. Nakamura, T. Uchijima, J. Nakamura, Surf. Sci. 383 (1997) 285.
[59] Y. Morikawa, K. Iwata, J. Nakamura, T. Fujitani, K. Terakura, Chem. Phys. Lett. 304 (1999) 91.